The European Journal of Research and Development

journals.orclever.com/ejrnd

OR CLEVER Science & Research Group

Research Article

Analytical Prediction and Experimental Validation of Bolt Self-Loosening under Vibration

Can İçmez[1*], Umut İnce[2], Samed Enser[3]

[1] Norm Fasteners, Orcid ID: https://orcid.org/0000-0002-9124-0100, e-mail: can.icmez@normfasteners.com
[2] Norm Fasteners, Orcid ID: https://orcid.org/0000-0002-3118-3060, e-mail: umut.ince@normfasteners.com
[3] Norm Fasteners (Present: Mehmet Akif Ersoy University) Orcid ID: https://orcid.org/0000-0002-6232-5498, e-mail: samedenser@mehmetakif.edu.tr
[*] Correspondence: can.icmez@normfasteners.com

Received: 02 June 2025
Revised: 23 October 2025
2nd Revised: 01 November 2025
Accepted: 02 December 2025
Published: 03 December 2025

Reference: İçmez, C., İnce, U., & Enser, S. (2025). Analytical prediction and experimental validation of bolt self-loosening under vibration. The European Journal of Research and Development, 5(1), 294–309.

Abstract

The self-loosening of bolted joints under vibrational loading remains a persistent challenge in many engineering applications, especially in the automotive industry, where safety and reliability are of paramount importance. Predicting self-loosening behavior is challenging because numerous parameters influence joint performance, as well as the limitations of conventional experimental testing. This study presents a novel analytical model for predicting bolt and nut loosening behavior under transverse vibration. The model extends existing approaches by incorporating additional parameters such as displacement, clamping force, and under-head friction torque. To enhance usability, the model was implemented in an MS Excel–based calculator with macro functions, enabling engineers to perform loosening analyses under varying conditions. The model adapts and extends existing approaches from the literature by incorporating an energy equilibrium approach, which calculates bolt rotation by balancing the torsional strain energy accumulated during vibration with the kinetic energy released once the applied torque exceeds the critical threshold. The analytical predictions were validated through Junker vibration tests, showing strong agreement with experimental data. The proposed model and tool provide a practical and accessible method for predicting loosening, thereby enabling the design of safer and more reliable fasteners while strengthening industrial competitiveness.

Keywords: Self-loosening, Fasteners, Vibration, Junker test, Analytical modeling

1. Introduction

Bolted joints are widely employed in the automotive, aerospace, energy, and civil sectors due to their simplicity and ease of disassembly. However, their reliability is often compromised by self-loosening under vibration, which can lead to preload loss, failures, and safety risks [1]. Among excitation mechanisms, transverse vibration is recognized as the primary cause of self-loosening. Junker's pioneering work [2], which later became standardized as DIN 65151, demonstrated that cyclic lateral displacement promotes slip at the under-head bearing surface and thread interfaces, causing progressive rotation and loss of clamp force. Subsequent investigations showed that loosening can initiate even under micro-slip conditions, where small relative motions accumulate rotation with each vibration cycle [3].

Further studies combined experimental and computational approaches to better capture the mechanics of loosening. Dinger and Friedrich [4] demonstrated that local slip zones under the bolt head and in the threads govern the onset of loosening, identifying critical displacement thresholds below 1 mm. These findings highlighted the importance of preload level, hole clearance, and friction coefficients in predicting loosening behavior.

Additionally, İnce and Güden [5] investigated the self-loosening behavior of bolted joints under cyclic transverse loading experimentally and numerically. Their study showed that existing analytical models could not fully predict the critical transverse displacement, achieving around 58 % accuracy. By introducing finite element–based parameters such as reaction moment and stiffness ratio, critical transverse displacement prediction accuracy improved to approximately 73 %, emphasizing the need for more comprehensive modeling approaches.

Analytical modeling has provided further insights into this problem. Nassar and Housari [6] presented a three-dimensional mathematical model to evaluate the effect of thread and under-head friction coefficients on loosening, implemented in MATLAB and validated experimentally. The results confirmed the central role of friction conditions in governing clamp force decay. Building on this, Nassar and Yang [7] developed an advanced formulation incorporating integral expressions for under-head torque, bolt bending effects, and critical slip forces. The model showed a strong correlation with measured torque–rotation curves, improving predictive accuracy.

More recently, Sun et al. [8] introduced a quantitative evaluation model that simplifies the problem to a single axis and defines two design criteria: an angular-acceleration criterion for loosening onset and a critical transverse load criterion. Their study compared bolts with spherical under-head geometries against standard bolts, both analytically and

experimentally, demonstrating enhanced resistance to loosening and illustrating the potential of geometry optimization.

Despite these advances, two limitations remain. First, most existing models require specialized software (e.g., MATLAB or finite element packages), which limits accessibility for engineers in practical design environments. Second, adaptability across various parameters, such as coatings, geometries, preload, and assembly conditions, remains limited without extensive re-derivation or numerical simulations.

To address these gaps, this work develops a parameter-adaptive analytical model for predicting bolt and nut loosening rates under transverse vibration. Unlike previous models, the formulation is implemented in an MS Excel–based calculator with macro functions, enabling engineers and technicians to perform loosening analyses across a variety of conditions without advanced coding or simulation tools. In addition, the proposed method introduces an energy equilibrium approach to determine the rotational motion of the bolt. In this approach, the torsional strain energy stored in the bolt during vibration is balanced against the kinetic energy released once the applied torque exceeds the critical torque threshold, allowing the angular displacement and loosening rate to be calculated analytically.

The model is validated through a series of Junker vibration tests, demonstrating strong agreement between analytical predictions and experimental data. The results confirm that the proposed approach accurately captures loosening behavior under different friction coefficients, preload levels, and head geometries. By reducing the need for extensive physical testing, the model shortens product development cycles, decreases testing costs, and promotes more sustainable design by lowering energy and resource consumption. Ultimately, this tool provides a practical pathway for designing safer and more reliable bolted joints while enhancing competitiveness in industries where fastener integrity is critical.

2. Materials and Methods

2.1. Loosening Mechanism of a Bolt

The clamping force generated by the tightening torque maintains the integrity of the bolted joint. However, when the joint is exposed to a transverse load that exceeds the frictional resistance created by this clamping force, relative motion begins to occur between the threads and at the interface under the bolt head.

Figure 1 illustrates the motion of the bolt when the upper plate moves in the x-direction. Figure 1Figure 1(1) shows the initial location of bolt and the plates. As the plate is displaced, it moves together with the bolt until reaching a critical slip point (δ_{crit}) (2). Beyond this point, the bolt begins to slide over the surface of the plate. The sliding

continues until the plate reaches its maximum lateral displacement (δ*) (3). The loosening of the bolt takes place between the critical slip point and the maximum displacement position.

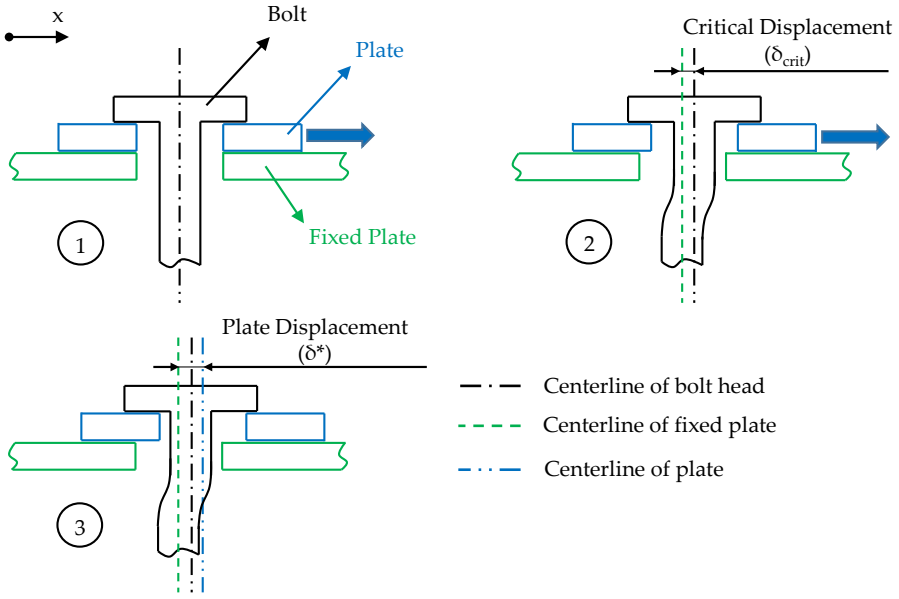

Figure 1: Transverse Displacement Behavior of the Bolt During Plate Motion in the x-direction

Figure 2 presents the time-dependent displacement of the plate. In Zone 1, the initial motion occurs as the plate moves from the zero position to its maximum position. Zones 2 and 3 represent the motion of the plate between successive maximum positions.

In this research, the loosening behavior of bolted joints under vibration was examined using the Junker test method, which is the most common approach for evaluating self-loosening performance. Originally developed by Gerhard Junker in 1969 [2], this method applies a controlled cyclic transverse displacement to a preloaded bolted joint while maintaining a constant clamping force. The test simulates real service conditions where bolts are exposed to vibration and lateral movement, such as in automotive or machinery applications. During the test, relative slip occurs between the bearing surface and the threads, causing a gradual reduction in the clamping force. The change in preload is continuously measured throughout the vibration cycles, allowing the loosening behavior to be monitored in real time. The typical result is a clamping-force-versus-cycle curve that shows an initial rapid decrease followed by a steady-state region, indicating the joint's resistance to loosening. Because it provides consistent and comparable results, the Junker test is widely used for evaluation and comparison of the anti-loosening performance of different fastener designs, coatings, and tightening conditions.

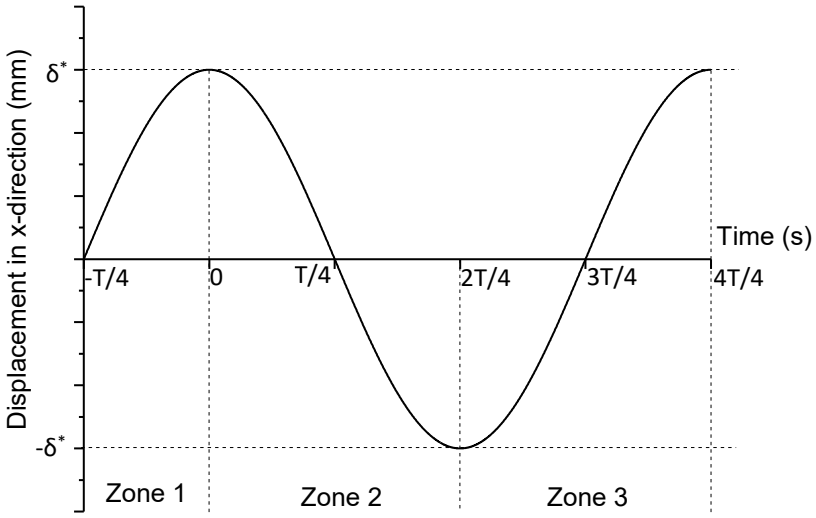

Figure 2: Time-Dependent Displacement of Plate in x-direction

2.2. Analytical Method for Calculation of Loosening Rate

During the bolt's complete cyclic displacement, shear friction forces acting on the bolt under-head and threads play an important role in the bolt's loosening behaviour. These forces are formulated by Nassar and Yang 2009 [7] along the x-direction as bearing friction shear force F_{bs} and thread friction shear force F_{ts}.

$$F_{bs} = \frac{3EI_1}{k \times L^3} \delta \sin(\omega t) \tag{1}$$

$$k = 1 - \left(\frac{3\lambda_b L}{4\lambda_b L + \frac{16EI_1 r_o}{\pi\left(r_o^4 - r_i^4\right)}} \right) \tag{2}$$

$$F_{ts} = F_{bs} \times \left[1 + \frac{\tan\alpha\, L}{\frac{r_{min}(\tau^4-1)}{2(\tau^3-1)} + \frac{1}{3} r_{maj} + 0{,}2725 \times P} \times \frac{\frac{8EI_1 r_o}{\pi\left(r_o^4 - r_i^4\right)} + \lambda L}{\frac{8EI_1 r_o}{\pi\left(r_o^4 - r_i^4\right)} + 2\lambda L} \right] \tag{3}$$

In this formulation, k represents the bending factor, E denotes Young's modulus of elasticity, and I_1 corresponds to the cross-sectional axial moment of inertia. The geometric parameters L, P, and α define the effective bolt length, thread pitch, and half of the thread profile angle, respectively. The contact dimensions under the bolt head are given by the outer radius r_o and inner radius r_i. Furthermore, δ indicates the transverse displacement of the plate, while ω stands for the angular velocity of the cyclic excitation. Finally, λ_b is

the constant for under-head bending stiffness, and τ represents the ratio of the major thread radius (r_{maj}) to the minor thread radius (r_{min}) ($\tau = r_{maj}/r_{min}$.).
These forces create torque, which stops the bolt's rotational movement.

$$T_{bs} = F_{bs} \times r_{be} \quad (4)$$

$$T_{ts} = F_{ts} \times r_{te} \quad (5)$$

Where r_{be} is the effective bearing radius and r_{te} is the effective thread radius.
If no loosening occurs during cyclic vibration, the frictional forces acting on the bolt are initially zero and increase sinusoidally as the transverse displacement grows, reaching their maximum amplitude at the point of maximum lateral movement. In this stage, the bolt and clamped parts move together without any relative slip, and the joint remains stable. However, once the applied transverse force exceeds the frictional resistance generated by the clamping load, a critical condition is reached. At this critical point, relative motion begins between the contacting surfaces, initiating the loosening process. Nassar and Yang [6] characterized this transition by defining the critical torques acting on the bolt — specifically, the under-head friction torque, the thread friction torque, and the pitch torque — which together determine the self-loosening. The relationship among these torques can be expressed as:

$$T_{bcr} = F \times \mu_b \times r_{be} \quad (6)$$

$$T_{tcr} = \frac{r_{te} \times \mu_t \times F \times \cos\beta \times \sqrt{\sec^2\alpha + \tan^2\beta}}{1 - \mu_t \times \sin\beta \times \sqrt{\sec^2\alpha + \tan^2\beta}} \quad (7)$$

$$T_p = \frac{F \times P}{2\pi} \quad (8)$$

Where T_p, T_{bcr} and T_{tcr} are pitch torque, torque of critical bearing friction and critical thread friction respectively. F is the clamp load, μ_b and μ_t are the bearing and thread friction coefficients, β, α and P are the lead helix angle, half of the thread profile angle and the thread pitch, respectively.
At the critical point T_{bs} reaches up until T_{bcr}. During this equilibrium, the bolt start to turn on the loosening direction with a net torque. Which can be expressed as:

$$T_{Net} = T_{ts} - T_{tcr} + T_p \quad (9)$$

Where T_{Net} is the net torque affecting the bolt to rotate in the loosening direction. This torque causes an angular acceleration on the bolt:

$$\alpha = \frac{T_{Net}}{I_2} \tag{10}$$

Where α is the angular acceleration and I_2 is the axial moment of inertia. This acceleration will later be used for the calculation of the bolt's loosening time.
In order to determine how much the bolt rotates, it is necessary to calculate its angular velocity. The kinetic energy equation was used to obtain this angular velocity. Until the bolt reaches the critical torque value, it is subjected to torsion. During this stage, torsional strain energy accumulates within the bolt, and once the applied torque exceeds the critical limit, this stored energy is suddenly released as kinetic energy, causing the bolt to rotate.

$$E_{Torsion} = T_0 \times \theta_0 \tag{11}$$

$$\theta_0 = \frac{T_0 \times L}{G \times J} \tag{12}$$

Where θ_0 is the angle of twist, L, G and J are the effective bolt length, the shear modulus and the polar moment of inertia, respectively. T_0 represents the residual torque remaining on the bolt, which was calculated from the torque–clamping force tests. It was obtained by multiplying the residual clamping load on the bolt by the experimentally determined T/F ratio.

$$T_0 = F \times \left(\frac{T}{F}\right)_{Exp} \tag{13}$$

Where F is the clamping load. T/F value was determined experimentally by applying torque in the loosening direction and may vary depending on the bolt type.
When the torsional strain energy reaches the critical torque value, it is converted into kinetic energy. This released energy causes the bolt to undergo rotational motion.

$$E_{Kinetic} = \frac{1}{2} \times I_2 \times \omega^2 \tag{14}$$

Considering the law of energy conservation, the accumulated torsional strain energy can be assumed to be equal to the kinetic energy of the bolt. Based on this equilibrium, the angular velocity of loosening can be determined.

$$E_{Torsion} = E_{Kinetic} \tag{15}$$

$$T_0 \times \theta_0 = \frac{1}{2} \times I_2 \times \omega^2 \tag{16}$$

$$\omega = \sqrt{\frac{2 \times T_0 \times \theta_0}{I_2}} \tag{17}$$

Using formulas 10 and 17, the time elapsed during the bolt loosening process can be calculated.

$$t_L = \frac{\omega}{\alpha} \tag{18}$$

Where t_L is the loosening time.
The following formulas were used to calculate the rotational angle of the bolt. The total loosening period was divided into ten equal intervals, and the rotation angle was calculated for each segment.

$$\Delta t_l = \frac{t_l}{10} \tag{19}$$

$$\omega_i = \omega_{i-1} + \alpha_i \times \Delta t_l \tag{20}$$

$$\theta_i = \theta_{i-1} + \omega_i \times \Delta t_l \tag{21}$$

$$\Delta\theta = \sum_{i=1}^{10} \theta_i \tag{22}$$

Each time the bolt reaches the critical torque value, it rotates by an angle of $\Delta\theta$. The rotation of the screw in the loosening direction causes a decrease in the clamping force, leading to vibration-driven self-loosening. The decrease in clamping force per degree of rotation was experimentally determined through testing. The experiments were carried out using the ST-Wrench, which measures the torque–angle relationship, and the vibration test device, which records the variation of clamp load with torque. In these tests, the assembly rigidity is the same as the assembly rigidity in vibration tests. In the procedure, the bolts were first tightened to the desired clamping load and then unscrewed to determine the reduction in clamp load per degree of rotation. By combining the results from both devices, the clamp load-angle relation was obtained. A total of six different parameter combinations were tested, consisting of two different clamp lengths and three different clamping loads. Three repetitions were performed for each

combination, resulting in a total of 18 tests. The resulting clamping load–angle relation of the tests is shown in Figure 3.

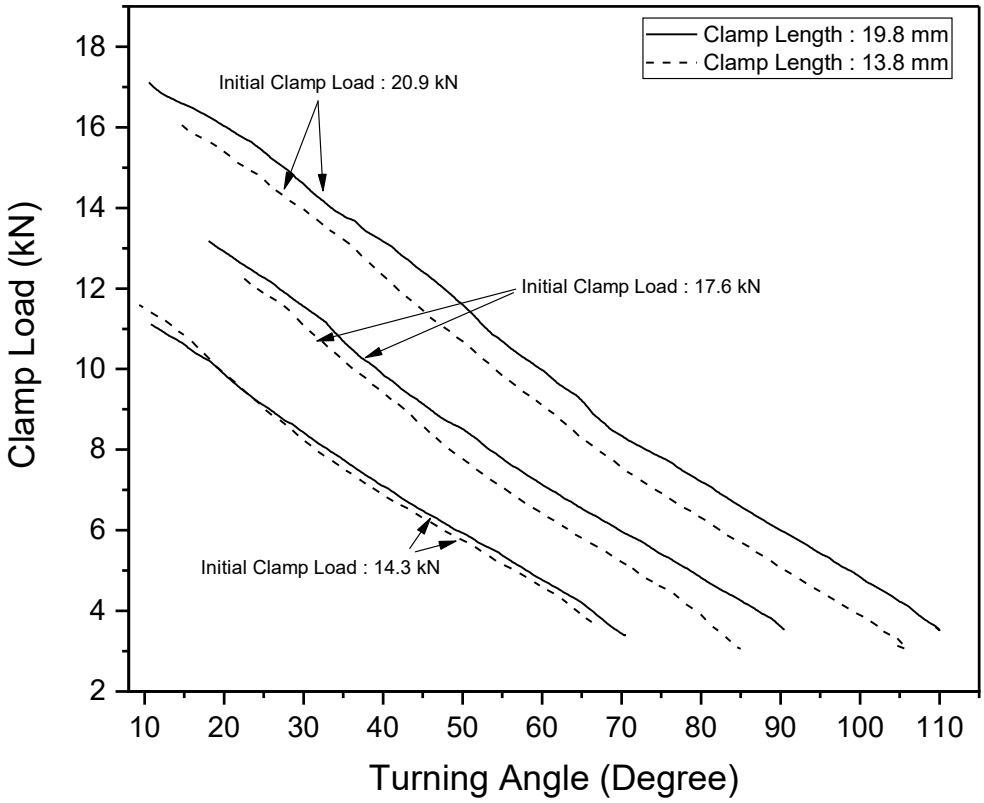

Figure 3: Clamping Load–Angle Relation of the Loosening Tests

Clamp load decrease per 1 degree of rotation is calculated with this formula:

$$\Delta F = \frac{\Delta\theta}{\phi^*} \tag{23}$$

Where ϕ^* is the slope of the angle–clamp load graph in Figure 3, and ΔF is the clamp load drop per 1 degree of rotation.

2.3. Experimental Analysis

Experimental tests were conducted using the Vibration Master J160 Junker test device shown in Figure 4. M8 DIN 933 bolts and DIN 934 nuts were used. The coatings of the bolts and nuts were chosen as KL100 with a VH301 top coat. The friction coefficient range was measured between 0.09 and 0.14.

Figure 4: Vibration Master J160 Junker Test Device

As shown in Table 1, eight different test variations were defined with two variables of three parameters: transverse displacement, clamping length, and clamping force. Transverse displacement values of 0.3 mm and 0.4 mm, clamping lengths of 13.8 mm and 19.8 mm, and clamping forces of 14.3 kN and 17.6 kN were selected. A total of 24 tests were performed, consisting of three repetitions for each of the eight parameter combinations.

Table 1. Variations Used for Junker Vibration Test

Test Variations [Var.]	Transverse Displacement [mm]	Clamp Load [kN]	Clamp Length [mm]
1	0.3	17.6	19.8
2	0.3	17.6	13.8
3	0.3	14.3	19.8
4	0.3	14.3	13.8
5	0.4	17.6	19.8
6	0.4	17.6	13.8
7	0.4	14.3	19.8
8	0.4	14.3	13.8

3. Results

The analytical model developed in this study was validated through Junker vibration tests conducted under various clamping forces and displacement amplitudes. M8 × 1.25 DIN 933 bolts and DIN 934 nuts with KL100 / VH301 GZ coatings were used.

Figure 5 and Figure 6 represent the comparison between experimental and analytically calculated results for clamping force reduction during transverse vibration at displacement amplitudes of 0.3 mm and 0.4 mm, respectively. In both cases, the analytical predictions successfully replicate the general trend of the experimental data, showing a rapid initial drop in clamp load followed by a more gradual decline toward stabilization. For the 0.3 mm transverse-displacement condition (Figure 5a and Figure 5b), the analytical model shows close agreement with the experimental curves for all parameter variations, with the maximum difference between predicted and measured loosening-rate values (kN/cycle) remaining within about ±10 %. In Figure 5a, which presents Variations 1 and 2, both analytical and experimental curves follow nearly parallel trends throughout the vibration cycles. Variation 1, corresponding to the higher clamping load (17.6 kN) and longer clamping length (19.8 mm), shows the smallest deviation, confirming that the model accurately represents the slower loosening rate caused by increased joint stiffness and preload. Variation 2, with a shorter clamping length (13.8 mm) but the same preload, exhibits a slightly faster clamp-load reduction, which is also well captured by the model. Figure 5b includes Variations 3 and 4 under the lower preload (14.3 kN) condition, where both experimental and analytical results indicate a more rapid loss of clamping force. Variation 3 loosens more slowly than Variation 4, again showing that higher stiffness improves vibration resistance.

For the 0.4 mm transverse-displacement condition (Figure 6a and Figure 6b), both analytical and experimental results show a more pronounced decrease in clamping force with increasing vibration cycles, confirming that greater displacement amplitude intensifies slip at the contact interfaces. In Figure 6a, which includes Variation 5 and Variation 6, the analytical and experimental trends exhibit similar overall shapes, though the analytical model slightly overestimates the remaining clamp load after about 150 cycles. Variation 5, characterized by higher preload (17.6 kN) and longer clamp length (19.8 mm), maintains the slowest loosening rate, whereas Variation 6, with a shorter clamp length (13.8 mm), demonstrates a faster decay in clamp force. In Figure 6b, corresponding to Variation 7 and Variation 8 with lower preload (14.3 kN), both sets of results show a steeper reduction in clamping force, consistent with higher energy release and greater slip per cycle. While the analytical predictions follow the general trend, they slightly over-predict the remaining clamping load at later cycles. This difference can be explained by neglected nonlinear effects such as dynamic friction changes and small surface slips between contact areas, which are not fully represented in the one-dimensional analytical model.

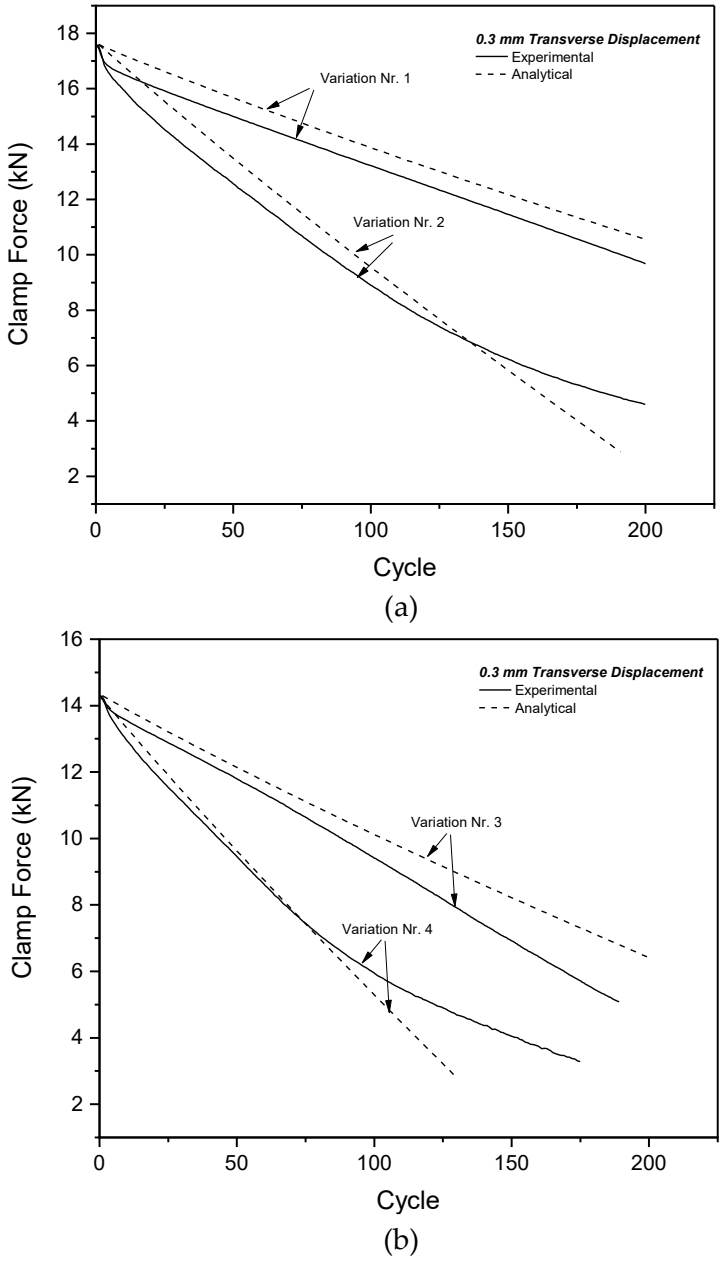

Figure 5: Experimental and Analytical Test Results for 0.3 mm Displacement for variation numbers (a) 1- 2 and (b) 3-4

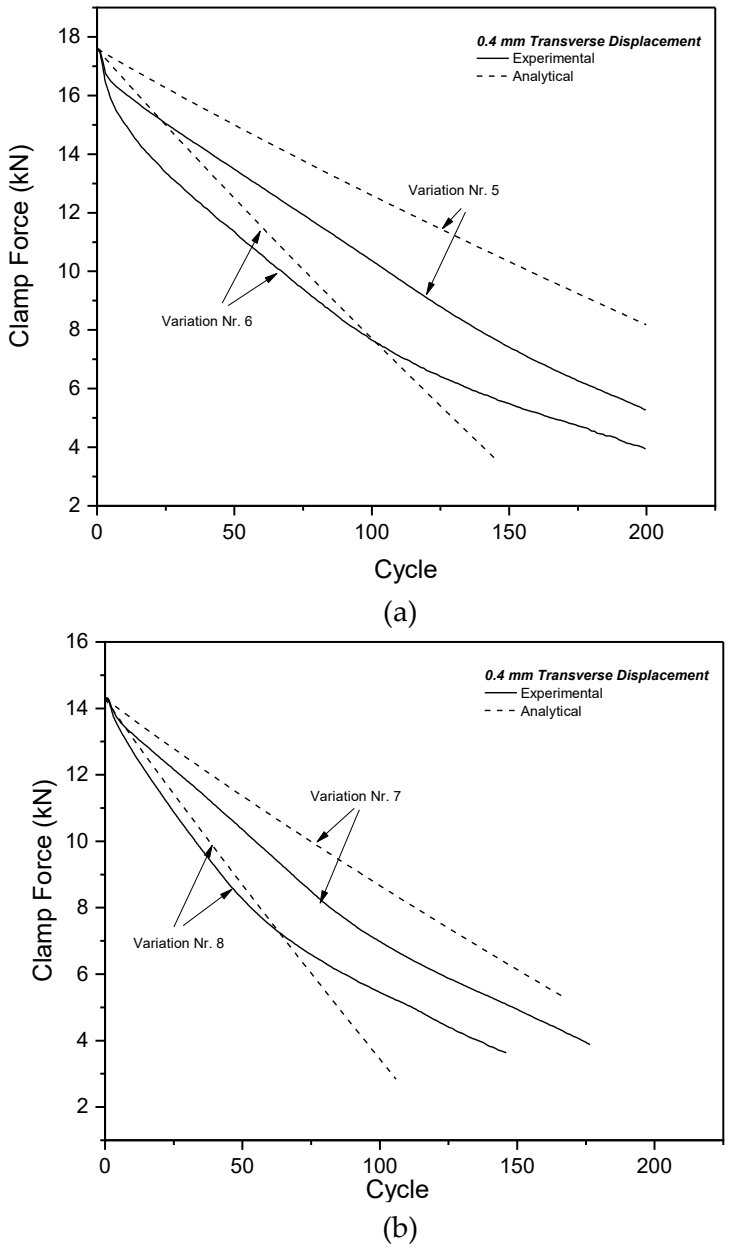

Figure 6: Experimental and Analytical Test Results for 0.4 mm Displacement for variation numbers (a) 5- 6 and (b) 7-8

Figure 7 presents the comparison between the calculated and experimentally measured loosening rates for all variations of the studied parameters. The results show a reasonable correlation between the analytical model and the experimental data, with most data points clustered around the unity line (Calc. LR / Exp. LR = 1), indicating well-correlated predictive accuracy. The deviations range from 1.2 % to 52.2 %, with an average deviation of 19.7 %.

The model demonstrates particularly good agreement for low and medium loosening rates (0.03–0.07 kN/cycle), where the ratio remains close to unity, validating the reliability of the energy-equilibrium formulation in this regime. Slight over-predictions are observed at higher loosening rates (> 0.07 kN/cycle), which are primarily associated with high-displacement (0.4 mm) and low clamping load (14.3 kN) conditions. This deviation can be attributed to the nonlinear slip behaviour and dynamic friction variation that are not fully captured in the simplified 1-D analytical formulation.

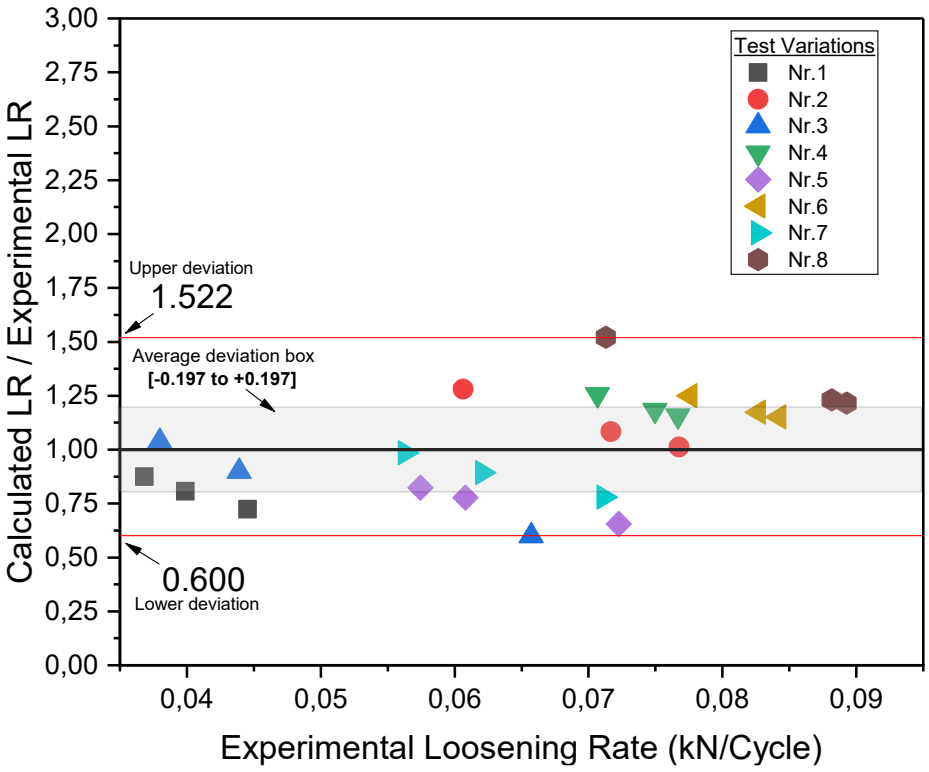

Figure 7: Accuracy of the Calculated Loosening Rate with respect to the Experimental Loosening Rate

4. Discussion and Conclusion

The presented results indicate that the adopted analytical model can accurately predict the loosening behaviour of bolted joints under transverse vibration. The comparison between the analytical calculations and the experimental Junker test results demonstrated reasonable agreement for different clamping forces, clamping lengths, and displacement amplitudes. The average deviation was approximately 19.7%, which is reasonable for preliminary design and analysis purposes.

The developed model reflects the influence of key parameters such as preload, clamp length, and displacement amplitude. Higher preloads and longer clamping lengths were shown to reduce loosening, while larger vibration amplitudes increased the loosening

rate. These trends are consistent with the physical mechanisms described in previous studies [5–8], confirming the reliability of the one-dimensional, energy-based approach.

The energy equilibrium method introduced in this study provides a practical means to estimate the bolt's rotation and loosening rate. The model assumes that when the critical torque is exceeded, all the stored torsional strain energy is instantly converted into kinetic energy. This assumption represents a fully elastic process, neglecting the portion of energy dissipated as heat through friction. Therefore, the observed deviations between the analytical and experimental results can partially be explained by this simplification.

Furthermore, the model uses a constant friction coefficient (within 0.09–0.14), while in reality, the friction coefficient may dynamically vary during vibration due to surface wear and micro-pitting. The absence of a dynamic friction model may contribute to the discrepancy between experimental and analytical outcomes, particularly at higher vibration amplitudes.

As expected, larger deviations were observed at higher loosening rates, which are associated with stronger dynamic effects, nonlinear contact behaviour, and possible limitations in the assumed energy conversion and friction conditions. Despite these effects, the general correlation between analytical predictions and experimental data remained reasonable across all test conditions.

The implementation of the model in an MS Excel–based calculator makes it accessible for engineers and technicians, even without advanced software or programming knowledge. The tool allows quick evaluation of loosening behaviour under different conditions, reducing the need for costly and time-consuming physical tests.

In conclusion, the proposed analytical model, supported by experimental validation, provides a simple yet effective method to predict the loosening rate of bolts under vibration. It offers a balance between accuracy and practicality, making it suitable for design and early testing stages in industrial applications. Future work will focus on applying the model to different bolt types and geometries, and on improving its accuracy by incorporating nonlinear friction effects. Overall, this study contributes to the development of safer, more reliable, and cost-effective bolted joint designs for automotive and other vibration-sensitive applications.

5. Acknowledge

The authors would like to thank Norm Fasteners for providing the laboratory facilities and technical support necessary to carry out the experimental studies.

References

[1] N. G. Pai & D. P. Hess (2002). Three-dimensional finite element analysis of threaded fastener loosening due to dynamic shear load. Engineering Failure Analysis, vol. 9, no. 4, pp. 383–402.

[2] G. Junker (1969). New criteria for self-loosening of fasteners under vibration. SAE Technical Paper 690055.

[3] N. G. Pai & D. P. Hess (2002). Experimental study of loosening of threaded fasteners due to dynamic shear loads. Journal of Sound and Vibration, vol. 253, no. 3, pp. 585–602.

[4] G. Dinger & C. Friedrich (2011). Avoiding self-loosening failure of bolted joints with numerical assessment of local contact state. Engineering Failure Analysis, vol. 18, no. 8, pp. 2188–2200.

[5] U. İnce & M. Güden (2021). An experimental and comparative study of the self-loosening of bolted joints under cyclic transverse loading. Sakarya University Journal of Science, vol. 25, no. 2, pp. 499–513.

[6] S. A. Nassar & M. Housari (2007). Effect of thread and bearing friction coefficients on vibration-induced loosening of bolted joints. Proceedings of the ASME International Mechanical Engineering Congress and Exposition (IMECE), Seattle, WA, USA, pp. 1–10.

[7] S. A. Nassar & X. Yang (2009). Mathematical modeling of vibration-induced loosening of bolted joints. Journal of Sound and Vibration, vol. 326, no. 3–5, pp. 713–729.

[8] Y. Sun, H. Zhang, & J. Zhang (2020). Quantitative evaluation of bolt self-loosening under transverse vibration. Proceedings of the Institution of Mechanical Engineers, Part C: Journal of Mechanical Engineering Science, vol. 234, no. 24, pp. 4929–4942.